JOURNAL OF GEOPHYSICAL RESEARCH, VOL. 116, D20124, doi:10.1029/2011JD016252, 2011

# A terrestrial gamma ray flash observed from an aircraft

D. M. Smith,[1,2] J. R. Dwyer,[3] B. J. Hazelton,[4] B. W. Grefenstette,[5] G. F. M. Martinez-McKinney,[1] Z. Y. Zhang,[1] A. W. Lowell,[2] N. A. Kelley,[1] M. E. Splitt,[6] S. M. Lazarus,[6] W. Ulrich,[7] M. Schaal,[3] Z. H. Saleh,[8] E. Cramer,[3] H. Rassoul,[3] S. A. Cummer,[9] G. Lu,[9] X.-M. Shao,[10] C. Ho,[10] T. Hamlin,[10] R. J. Blakeslee,[11] and S. Heckman[12]

Received 16 May 2011; revised 2 August 2011; accepted 3 August 2011; published 27 October 2011.

[1] On 21 August 2009, the Airborne Detector for Energetic Lightning Emissions (ADELE), an array of six gamma-ray detectors, detected a brief burst of gamma rays while flying aboard a Gulfstream V jet near two active thunderstorm cells. The duration and spectral characteristics of the event are consistent with the terrestrial gamma ray flashes (TGFs) seen by instruments in low Earth orbit. A long-duration, complex +IC flash was taking place in the nearer cell at the same time, at a distance of ~10 km from the plane. The sferics that are probably associated with this flash extended over 54 ms and included several ULF pulses corresponding to charge moment changes of up to 30 C km, this value being in the lower half of the range of sferics associated with TGFs seen from space. Monte Carlo simulations of gamma ray propagation in the Earth's atmosphere show that a TGF of normal intensity would, at this distance, have produced a gamma ray signal in ADELE of approximately the size and spectrum that was actually observed. We conclude that this was the first detection of a TGF from an aircraft. We show that because of the distance, ADELE's directional and spectral capabilities could not strongly constrain the source altitude of the TGF but that such constraints would be possible for TGFs detected at closer range.

**Citation:** Smith, D. M., et al. (2011), A terrestrial gamma ray flash observed from an aircraft, *J. Geophys. Res.*, *116*, D20124, doi:10.1029/2011JD016252.

## 1. Introduction

[2] A total of well over a thousand terrestrial gamma ray flashes (TGFs) have been detected from space, first by the Burst and Transient Source Experiment (BATSE) on the Compton Gamma-Ray Observatory (CGRO) [*Fishman et al.*, 1994], and more recently by the Reuven Ramaty High Energy Solar Spectroscopic Imager (RHESSI) [*Smith et al.*, 2005], the Fermi Gamma-ray Burst Monitor (GBM) [*Briggs et al.*, 2010], and the Astro-rivelatore Gamma a Immagini Leggero (AGILE) [*Tavani et al.*, 2011]. TGFs are associated with thunderstorms [*Fishman et al.*, 1994] and, indeed, individual lightning flashes [*Inan et al.*, 1996; *Cummer et al.*, 2005; *Cohen et al.*, 2006; *Inan et al.*, 2006; *Connaughton et al.*, 2010], with most classifiable atmospherics (sferics) suggesting positive intracloud (+IC) flashes, including some narrow bipolar events (NBEs), as the type of parent lightning [*Stanley et al.*, 2006; *Shao et al.*, 2010; *Lu et al.*, 2010, 2011]. TGFs are extraordinarily bright events, although usually less than 1 ms in duration, often saturating the counting capabilities of orbiting gamma ray detectors even from a distance of over 600 km away [*Grefenstette et al.*, 2007, 2009]. Approximately $10^{17}$ relativistic electrons, and a comparable number of their bremsstrahlung gamma ray photons, are calculated to be produced in a TGF [*Dwyer and Smith*, 2005]. The energy spectrum of TGF photons has been shown to be comparable to the expectation for a relativistic

[1]Santa Cruz Institute for Particle Physics, Physics Department, University of California, Santa Cruz, California, USA.
[2]Space Sciences Laboratory, University of California, Berkeley, California, USA.
[3]Department of Physics and Space Sciences, Florida Institute of Technology, Melbourne, Florida, USA.
[4]Department of Physics, University of Washington, Seattle, Washington, USA.
[5]Space Radiation Laboratory, California Institute of Technology, Pasadena, California, USA.
[6]Department of Marine and Environmental Systems, Florida Institute of Technology, Melbourne, Florida, USA.
[7]National Weather Service, Key West, Florida, USA.
[8]Department of Medical Physics, Memorial Sloan-Kettering Cancer Center, New York, New York, USA.
[9]Electrical and Computer Engineering Department, Duke University, Durham, North Carolina, USA.
[10]Los Alamos National Laboratory, Los Alamos, New Mexico, USA.
[11]NASA Marshall Space Flight Center, Huntsville, Alabama, USA.
[12]AWS Convergence Technologies, Inc., Germantown, Maryland, USA.


0148-0227/11/2011JD016252

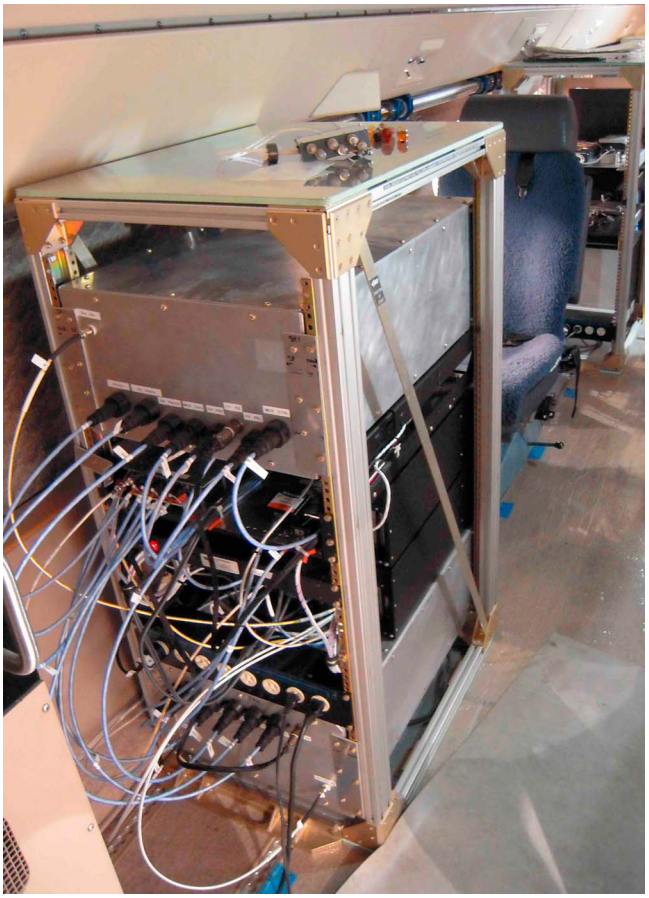

**Figure 1.** ADELE installed in the GV. The aluminum boxes at top and bottom are the sensor heads; the two computers are the black boxes in the middle of the rack.

runaway avalanche [*Dwyer and Smith*, 2005; *Carlson et al.*, 2007; *Babich et al.*, 2008; *Hazelton et al.*, 2009].

[3] Observations of gamma rays from thunderstorms have been made near their altitude of origin by instruments on balloons [*Eack et al.*, 1996a, 1996b] and aircraft [*Parks et al.*, 1981; *McCarthy and Parks*, 1985] but no TGFs were reported by these authors, only events of much longer duration, probably much fainter, that do not have an analog in observations from space. Since those instruments were built before the discovery of TGFs, they may not have been designed with the high time resolution and throughput (maximum count rate) needed for TGF detection.

## 2. Instrument and Data

[4] The Airborne Detector for Energetic Lightning Emissions (ADELE) is a set of gamma ray detectors designed to study the TGF phenomenon at close range as well as other manifestations of high-energy radiation in thunderstorms. ADELE was completed in the spring of 2009 and flown above and around thunderstorms in the continental United States, mostly Florida, in August 2009, on the Gulfstream V (GV) jet operated by the National Center for Atmospheric Research (NCAR) on behalf of the National Science Foundation (NSF).

[5] ADELE's detectors are designed to cover the largest possible dynamic range in incoming flux, since a TGF that produces 100 counts in a detector at 600 km in low Earth orbit would produce $10^6$ counts in the same detector only 6 km above the event, if the effects of atmospheric absorption were the same. While it would be difficult to design a detector that can count $10^6$ events in a millisecond, we chose a strategy that would allow us to cover the full likely dynamic range without saturation, even if fewer counts are collected. ADELE uses three kinds of scintillator, each optimized for a different range of photon flux. There is one of each type of detector in two sensor heads, one at the top and one at the bottom of an instrumentation rack that takes the place of a seat inside the GV (Figure 1). A sheet of 1/8″-thick lead is bent around the bottoms of the detectors in the upper sensor head and around their tops in the lower, to provide a rough directionality in ADELE's response to photons below about 400 keV.

[6] In each sensor head, a cylindrical NaI scintillator (5″ in diameter and 5″ long) provides good stopping power. In these detectors, Compton scattering of an incoming gamma ray is usually followed by photoelectric absorption so that the full energy is deposited and recorded, with good energy resolution (<10% FWHM at 662 keV). The NaI detectors will saturate at count rates beyond ~$10^5$ Hz. These detectors are read out by direct flash digitization of the signal from the phototube with a Gage Octopus™ PCI card sampling at 12.5 MHz. These data are continuously recorded in a circular buffer on the card but are only read out to the computer during occasional 1 s intervals triggered by high count rates in the plastic detectors (see next paragraph). A flat-plate antenna mounted on the bottom of the aircraft, measuring $dE/dt$, is digitized simultaneously in another channel of the Gage card. The TGF we discuss in this paper was unfortunately not bright enough to trigger sampling of the NaI and flat-plate data.

[7] Each sensor head also contains a 5″ × 5″ plastic scintillator and a 1″ × 1″ plastic scintillator, the latter designed to return good data if the larger detector saturates. Due to the fast decay of the light signal in the BC-408 plastic used, the count rate in these detectors is limited by the response time of the phototubes and our electronics, allowing up to a 3 MHz count rate in each detector. The signal from the phototubes is sent to a network of clamping amplifiers (to cope with overloads from cosmic rays) with no shaping, and the amplified signals are split out to four discriminators, which were set during these flights to voltages corresponding to deposited energies of ~50 keV, 300 keV, 1 MeV and 5 MeV. While crude, this energy binning allows us to distinguish, for example, between the lower-energy spectrum associated with stepped leaders seen from the ground and the higher-energy spectrum usually associated with TGFs. Crude energy discrimination is also well matched to plastic detectors, which not only have poorer light yield and therefore energy resolution than NaI, but also tend to Compton scatter gamma rays out of the detector volume, collecting only a fraction of their energy, rather than absorbing all of it. This process is modeled by Monte Carlo computer simulations in order to compare model spectra with data from the plastic detectors (see section 3.4). This process is also necessary for all other TGF detectors, but not to as great a degree.

[8] Each discriminator produces a continuous output voltage at one of two discrete levels, depending on whether the voltage from the amplified photomultiplier signal is

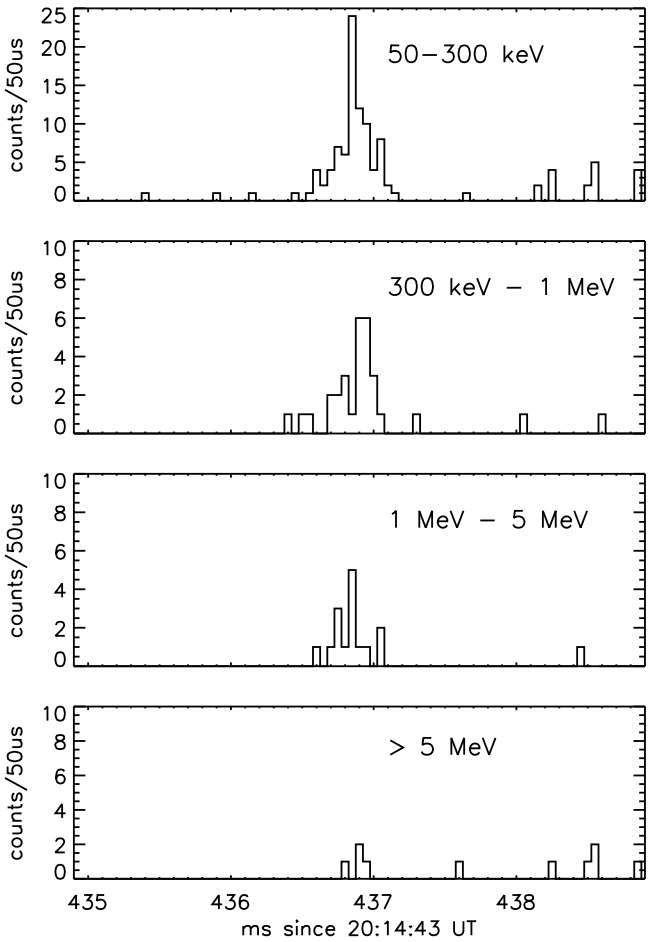


**Figure 2.** Time profile (counts per 50 $\mu$s) of the TGF recorded on 21 August 2009 at 20:14:43.437 UT. The counts shown are summed over both large plastic detectors. The breakdown of counts by energy channel and detector is shown in Table 1.

above or below that discriminator's threshold. Each pulse coming out of the detector, if it is large enough, therefore creates one rising edge and one falling edge in the output of the discriminator, with the discriminator output remaining high in between. This bilevel output of the discriminators is sent out of the sensor head to a field-programmable gate array (FPGA) board in a tray between the sensor heads in the instrument rack, just above the instrument computers. The FPGA samples the signals from the discriminators at 200 MHz, counting both rising edges (giving count rate in each integral channel) and high samples (giving a measure of dead time, since a new pulse cannot be counted before the last one has decayed). These counts are accumulated in 50 $\mu$s intervals, and the accumulations are formed into data packets that are transmitted via an ethernet interface to the primary instrument computer. The FPGA uses the one-pulse-per-second signal from a GPS receiver to label the 50 $\mu$s bins relative to the absolute integer second marks, and the primary computer, which is synchronized to GPS at the start of each flight, marks the packets with the time itself. The secondary computer holds the Gage flash board and reads out its data when it is triggered by the primary computer, based on a realtime analysis of the incoming data from the large plastic detectors.

[9] The first ADELE test flight took off from Rocky Mountain Municipal Airport on 7 August 2009 and continued on toward thunderstorm activity in Montana. After a ferry flight of the GV to Melbourne, Florida, eight more ADELE flights took place from that airport, all pursuing storms within or near Florida, from 16 August through 2 September. ADELE was in the air and operating for a total of ~37 h for this set of flights.

## 3. Results

### 3.1. TGF Observation

[10] In a previous paper [*Smith et al.*, 2011] we noted that ADELE flew within 10 km of lightning identified via 1213 distinct sferics measured by the Weatherbug Total Lightning Network (WTLN), the United States Precision Lightning Network (USPLN), and the National Lightning Detection Network (NLDN) without seeing any gamma ray signal large enough to be discriminated effectively from the background count rate due to cosmic ray secondary photons. We concluded that TGFs of the intensity seen from space are rare at altitudes of 9 km and higher, appearing with fewer than 1% of lightning flashes.

[11] Only one event was seen by ADELE that has the two defining empirical characteristics of a typical TGF seen from space: a duration of slightly less than 1 ms and significant spectral content above 1 MeV. Figure 2 shows the time profile of this event in the native 50 $\mu$s bins of the plastic data mode, in four energy channels: 50–300 keV, 300 keV to 1 MeV, 1–5 MeV, and >5 MeV. These channels are made by subtracting the counts in the raw integral channels to make differential ones. These profiles are summed over both large plastic detectors. The event was too faint either to register significantly in the small plastic detectors or to trigger data collection by the NaI detectors in triggered mode. Table 1 gives the number of counts in each integral energy channel of each large plastic detector along with the background level per millisecond due to gamma rays associated with the nearly constant cosmic ray input to the atmosphere and the plane.

[12] This event occurred at 20:14:43.437 UT on 21 August 2009, with the plane at latitude 31.0746° and west longitude 81.5453°, over coastal estuaries on the southeast coast of Georgia near the town of Brunswick. The GV was at 14.1 km, a typical cruising altitude during the ADELE flights. Figure 3 shows a map of all WTLN sferics within 5 min of the TGF. The plane, moving from left to right, had recently emerged from flying through the top of a very active cell, and was about to pass near an even more active one. Four flashes from the edge of the second cell are very near the plane's position at the time of the TGF, although none of them corresponds to the TGF, the closest in time being 34 s afterward, when the plane had already reached the other end of the second cell.

### 3.2. Radio Observations

#### 3.2.1. Observations of This Event

[13] Near the center of this second cell was a discharge that was observed by WTLN and NLDN at 20:14:43.426 UT, 11 ms before the TGF time. Both positions are marked in

**Table 1.** Large Plastic Detector Counts in Each Integral Energy Channel for the TGF of 21 August 2009[a]

| Detector | Channel 1 >50 keV | Channel 2 >300 keV | Channel 3 >1 MeV | Channel 4 >5 MeV |
|---|---|---|---|---|
| Upper | 77 (3.5) | 26 (0.83) | 9 (0.52) | 3 (0.44) |
| Lower | 52 (4.2) | 18 (0.91) | 10 (0.60) | 1 (0.51) |

[a]Background per millisecond in parentheses.

Figure 3 and are in good agreement; averaging the positions gives a distance of 10.3 km from the plane. This discharge was identified as +IC by NLDN and examination of the WTLN waveform confirms this classification.

[14] Figure 4 shows broadband magnetic data from the Duke University sensors near Durham, NC, 580 km from ADELE (or 2 ms of light propagation delay). The sferic used by NLDN and WTLN to locate this flash is labeled event 1 in Figure 4 (top), which shows data from a sensor sensitive from 100 Hz to 25 kHz. Figure 4 shows the horizontal magnetic field from the crossed sensors broken into components perpendicular (blue) and parallel (red) to the line of sight between Durham and the region containing ADELE and the two nearby cells. Sferics dominated by $B_\phi$, the perpendicular component, are consistent with an origin in that direction. Seven more sferics from the same direction, labeled 2–8 in Figure 4, extend over the 54 ms following the first +IC sferic. We believe it likely that this sequence represents causally connected discharges that are part of a single flash. On this plot, the time axis is corrected by 2 ms so that sferics coming from the TGF region are at their actual time of occurrence at the source region; the TGF therefore occurs about 3 ms before the small sferic 2. The three sferics marked with an "X" in Figure 4 (top) show significant radial $B$ in this coordinate system, and are therefore coming from a significantly different direction and are not related to this storm.

[15] Figure 4 (bottom), the ULF magnetic data from Durham, shows four strong, slower currents (2–5) associated with the discharges just after the TGF. These have considerably more ULF power than the strongest VLF pulse (1), which begins the sequence. *Lu et al.* [2010, 2011] found that TGFs are often associated with +IC discharges with considerable ULF energy, and sometimes several VLF pulses. The charge moment change associated with the largest slow ULF pulse (5) is 30 C km, which is greater than the value derived for 15 out of 54 RHESSI TGFs studied by *Lu et al.* [2011], who found a median charge moment change of 46 C km for their sample. Close examination of the ULF data shows that there was no cloud-to-ground (CG) channel within 30 km of this discharge in a 4 s window centered on the TGF; thus, this sequence of discharges makes up part of a purely IC flash, in agreement with the WTLN and NLDN identifications.

[16] This chain of VLF pulses (1 to 8) is not unusually long for a +IC flash, but it is unusual to see a train of ULF pulses, indicating long-duration upward negative charge transfer. We suggest that this part of the signal might be produced by a sequence of K processes recurring along upward leader channels established earlier. The TGF may have been produced during the initial progression of this leader, which followed the initiation event recorded by WTLN and NLDN. The timing of the TGF, coming well after the initiation sferic, demonstrates that the TGF is not the initiating mechanism for the flash.

[17] While none of the sferics observed from Duke were simultaneous with the TGF, a single station of the Los Alamos Sferic Array (LASA) at Tallahassee, Florida, saw a small sferic (Figure 5), consistent with a +IC discharge, overlapping the time of the TGF, assuming it originated at the TGF's location. These electric field data are not corrected for light propagation (0.9 ms), so the sferic between 437.8 ms and 438.0 ms is the one corresponding to the TGF's occurrence time. No other sensor, LASA, Duke, or commercial, appears to have seen this discharge. The association cannot be proven, since the sferic was not geolocated. The Tallahassee station triggered not on the event itself but on a local interference source. If the discharge is assumed to be at the position of ADELE, the waveform can be used to derive an ionospheric height of ~60 km, a reasonable daytime value. This is only suggestive and by no means proof that this sferic was related to the gamma ray event. Whether other sensors should have been expected to see the event recorded by LASA/Tallahassee is difficult to determine. The sensors are of different types (electric versus magnetic), and the LASA sensor may have been particularly sensitive to this event since the signal is very impulsive, LASA has a high bandwidth, and the event occurred close to the station (~270 km), so long-distance propagation had no chance to filter out the highest frequencies.

### 3.2.2. Comparison With Other TGFs in Radio

[18] We would like to determine if the association of a TGF with a very small VLF signal, either alone or as part of a flash having larger VLF pulses, is consistent with previous observations of TGFs.

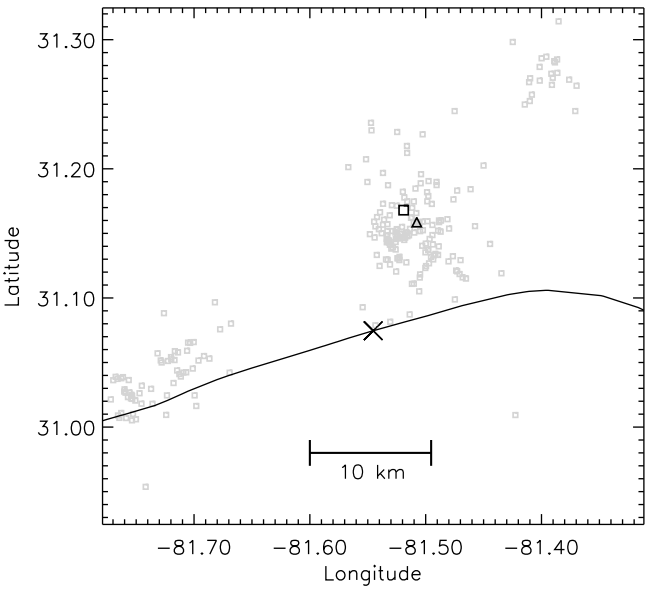


**Figure 3.** Lightning data (gray squares) from WTLN within 5 min of the TGF of 21 August 2009. The black line is the track of the plane, and the "X" marks its position at the time of the TGF. The +IC sferic occurring 11 ms before the TGF is marked by a square (the NLDN position) and a triangle (the WTLN position).

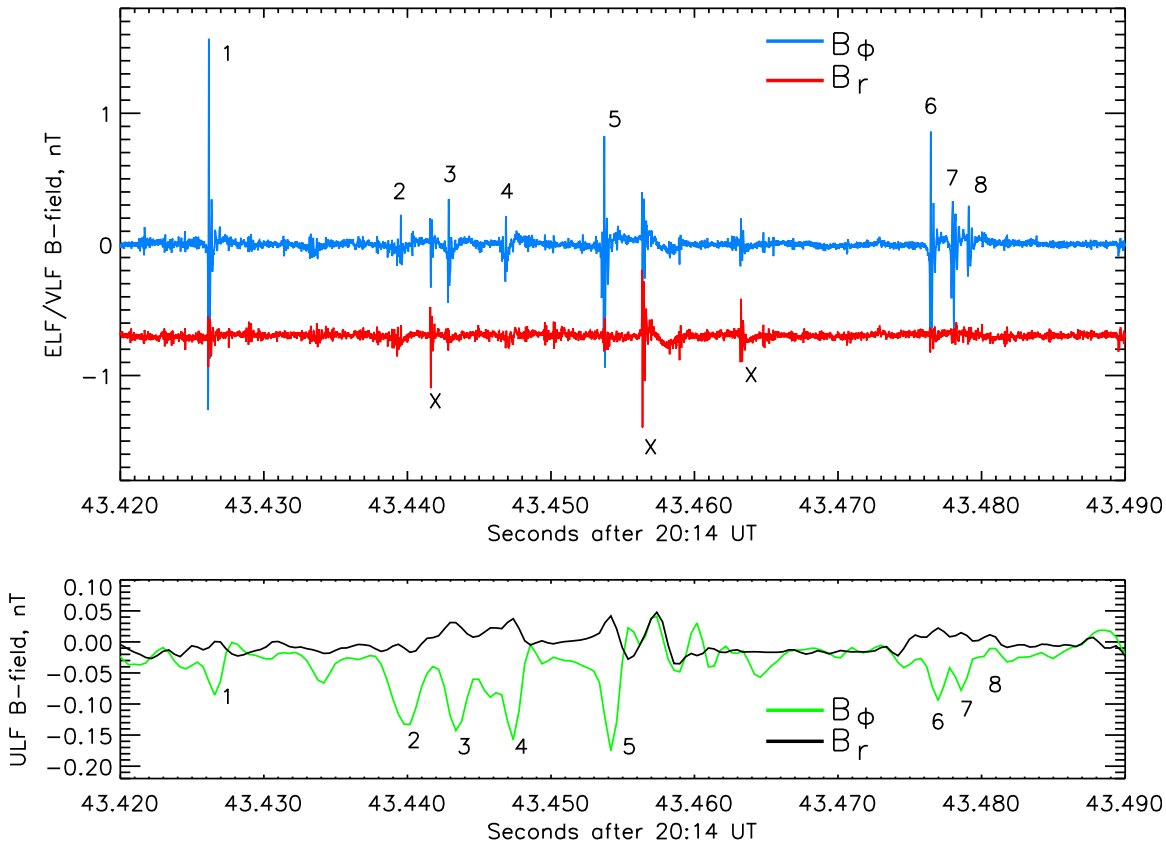


**Figure 4.** The sequence of sferics observed by the Duke University sensors near Durham, North Carolina. The sferics marked 1–8 show magnetic field excursions only in the direction perpendicular to the vector toward ADELE and are thus consistent with an origin in the storms shown in Figure 3, while the sferics marked with an "X" originate from other directions. (top) ELF/VLF signal. (bottom) ULF signal. Time is corrected for light propagation to ADELE's position, so the TGF occurred between sferics 1 and 2.

[19] Sferics with several VLF pulses are common in the TGF literature [*Stanley et al.*, 2006; *Cohen et al.*, 2006; *Shao et al.*, 2010; *Cohen et al.*, 2010; *Lu et al.*, 2010; *Connaughton et al.*, 2010; *Lu et al.*, 2011; *Cummer et al.*, 2011]. All these results except *Cohen et al.* [2006], *Connaughton et al.* [2010], and *Cummer et al.* [2011] use TGFs from RHESSI and are subject to the ~2 ms uncertainty in its clock [*Grefenstette et al.*, 2009]. In the newest results from Fermi, *Connaughton et al.* [2010] examined the timing relationship between Fermi TGFs and VLF sferics from the World Wide Lightning Location Network (WWLLN). They found sferics associated with 15 out of 50 Fermi TGFs. For most of these events, the sferic occurred within 100 $\mu$s of the peak of the gamma ray emission. But for one of their matches, the sferic came almost 4 ms after the TGF, and for another it came almost 3 ms before the TGF. It is quite possible that in these events, like in ours, the discharge corresponding to the TGF was not the one with the greatest VLF power in the flash.

[20] There is also nothing in the literature to rule out a subpopulation of TGFs with extremely weak radio emission overall. Of course any of the 35 Fermi events not matched to WWLLN could have had extremely small corresponding VLF signals. The highest rate of matching VLF sferics to TGFs has been achieved by the Stanford network of receivers, including the very low background installation at Palmer Station, Antarctica, with an atmospheric noise level of ~0.1 pT corresponding to <3 kA at 10 Mm [*Inan et al.*, 2006] for CG lightning. Using these receivers, *Cohen et al.* [2010] found matches for all but 9 out of 158 RHESSI TGFs. *Lu et al.* [2011] found VLF sferics exceeding five times the local noise level for the Duke sensors (20 pT) in 56 out of 78 or 72% of RHESSI TGFs studied, showing that TGFs without a sferic strong enough to register with these sensors are not uncommon.

[21] Taking all the literature together, our event, with the TGF appearing in the middle of a series of VLF pulses at a time with either no pulse or with a very small and/or impulsive one, does not seem necessarily anomalous.

### 3.3. Meteorological Context

[22] The cell that produced the TGF was part of a line of convective cells that formed in the region of a collision between the sea breeze boundary and a southeastward moving outflow boundary from convection that had dissipated to the northwest. Figure 6 is an east-to-west vertical cross section of reflectivity from the Jacksonville NEXRAD radar (KJAX), at the latitude of the TGF at 20:13 UT, covering 70 km in the east/west direction. There appears to be an updraft near the center of the plot, corresponding roughly

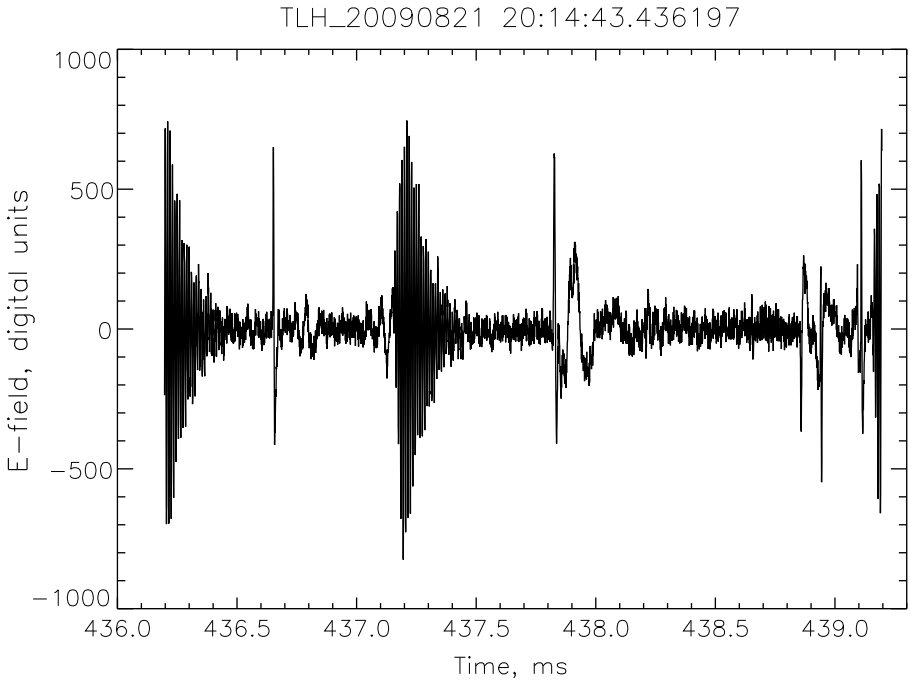


**Figure 5.** Electric field data from the LASA station in Tallahassee, Florida, during the TGF of 21 August 2009. The small +IC sferic consistent with the TGF timing and distance appears between 437.8 and 438.0 ms. The noise source that triggered the array can be seen at 436.2 and 437.2 ms.

to the TGF position, overshooting a larger, stable layer of reflectivity (precipitation) at about 14 km.

[23] The cell that produced the TGF was almost midway through its electrical development as represented by production of sferics. Figure 7 shows a time history of the number of sferics in the cell that produced the TGF, shown in Figure 3, binned into 15 s intervals, with the time of the TGF marked in red. About a minute later, there is a ~2 min gap. While this could easily be coincidental, we note that the train of ULF pulses immediately following the TGF, combined with the large number of other discharges in the following minute, may have temporarily drained the charge structure of the storm well below its equilibrium level through the rest of the cell's activity. *Smith et al.* [2010] found that TGFs tend to occur in the declining phase of the associated storm. In this case, we don't know if the cell produced other TGFs at other times in its development because the plane was not in range.

### 3.4. Interpretation of Gamma Ray Data

[24] In Figure 1 of *Smith et al.* [2010], reproduced here as Figure 8, we show the expected number of counts ADELE would see from a typical TGF emitting $10^{17}$ gamma rays. The counts are summed over both large plastic detectors in the >300 keV channel, and the contours show the location of the TGF in altitude (absolute) and in radial distance relative to the plane's location. The plane is assumed to be flying between 14.0 and 14.5 km.

[25] These contours are generated by a three-stage Monte Carlo simulation described in more detail by *Smith et al.* [2010]. Similar simulations of the detectability distance of

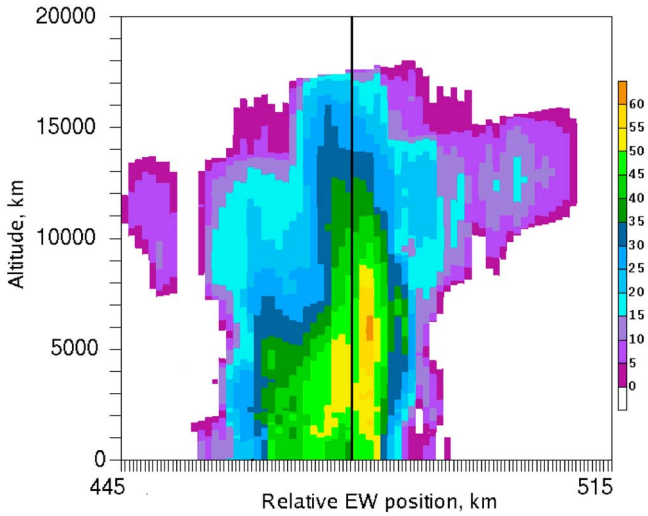


**Figure 6.** Image of radar reflectivity (color scale in dBZ). The *y* axis is altitude in meters, and the *x* axis is east/west position in kilometers; the 460 km point represents the longitude of the Jacksonville radar (−81.70194°). The slice is made along a line 76 km north of the radar latitude (30.48444°), passing through the position of the IC flash we believe is associated with the TGF. The TGF position, taken as the average of the WTLN and NLDN positions from Figure 3, is shown as a vertical black line, falling within a zone of enhanced reflectivity above 14 km.

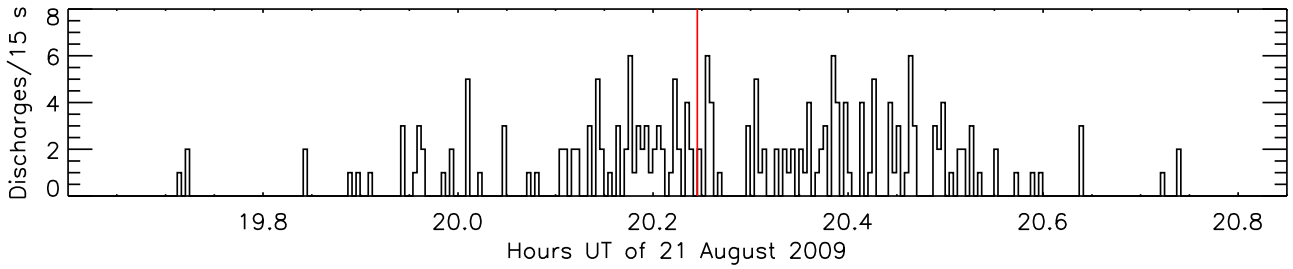


**Figure 7.** Histogram showing the number of USPLN sferics in 15 s intervals from the cell producing the TGF. The time of the TGF is shown as a vertical red line.

TGFs from aircraft have been performed by *Hansen et al.* [2010], with similar results.

[26] In the first stage, the TGF itself is simulated, and normalized to produce a beam of $10^{17}$ gamma rays from 20 keV to 50 MeV with an angular distribution and energy spectrum determined by the relativistic runaway avalanche process [*Dwyer*, 2007]; the energy spectrum is shown in Figure 9 (top). The simulated avalanche region is a zone of high, constant, downward electric field (400 kV/m sea level equivalent) extending over 87 g cm$^{-2}$ of atmosphere downward from its high-altitude end point. The vertical extent of the field region in kilometers is therefore a function of the atmospheric density, being more compact at lower altitudes. As an example, we show in Figure 9 (bottom) the altitude distribution of the gamma rays when the upper end of the field region is at 12 km and the lower end is at 9.7 km. The TGF altitude shown as the *y* axis in Figure 8 is the upper end of the field region; as Figure 9 (bottom) shows, this is where most gamma rays are produced. The second and third stages of the simulation propagate the TGF gamma rays first through the intervening atmosphere and then through the aircraft and ADELE detectors.

[27] ADELE's sensitivity limit of 20 counts >300 keV, the outer contour in Figure 8, corresponds to 0.14 photons cm$^{-2}$ at the aircraft and is defined by our ability to distinguish a real signal from Poisson fluctuations in the background count rate. It is apparent from Figure 8 that this limit occurs quite close to a radial distance of 10 km for TGF source altitudes ranging from 10–20 km. Table 1 shows that we saw 44 counts above >300 keV (42 if background is subtracted), or about twice the predicted value for an ordinary TGF at 10 km distance. Thus the combined gamma ray and sferic data show this event to be consistent within a factor of 2–3 with the typical luminosity derived from observations of TGFs from space, if the TGF source was indeed at the position of the temporally associated +IC flash. We might expect the first TGF we see to be near our sensitivity limit, since the observed intensity is a function of radial distance, and the plane is most likely to be in an annulus of the largest possible radius when the event occurs.

[28] We have two other pieces of information that can help us constrain the intrinsic brightness, production altitude, and distance of the ADELE TGF: the spectral distribution and top/bottom ratio of counts given in Table 1. From Table 1, the top-to-bottom ratio above 300 keV (background subtracted) is 1.47, lying between 0.70 to 3.21 with 95% confidence. To take advantage of spectral information, we subtract channel 3 from channel 2 to make a differential energy channel from 300 keV to 1 MeV and compare it to channel 3 (integral counts above 1 MeV). Summed over top and bottom detectors and background subtracted, the ratio (300 keV to 1 MeV)/(>1 MeV) = 1.36, with a 95% confidence interval of 0.64–2.85. While these are not strong constraints due to the limited number of counts available, we examine whether we can exclude certain values for the TGF's source altitude and radial distance.

[29] We do not make use of the lowest energy channel (>50 keV) in these ratios because we have observed that cosmic rays, which can deposit ~25 MeV or more in the plastic detectors, sometimes trigger more than one count in the channel 1 discriminators. It is unlikely, but not impossible, that some of the TGF photons may also have triggered a double count in this lowest channel. ADELE's electronics have been modified to eliminate this problem in future flights.

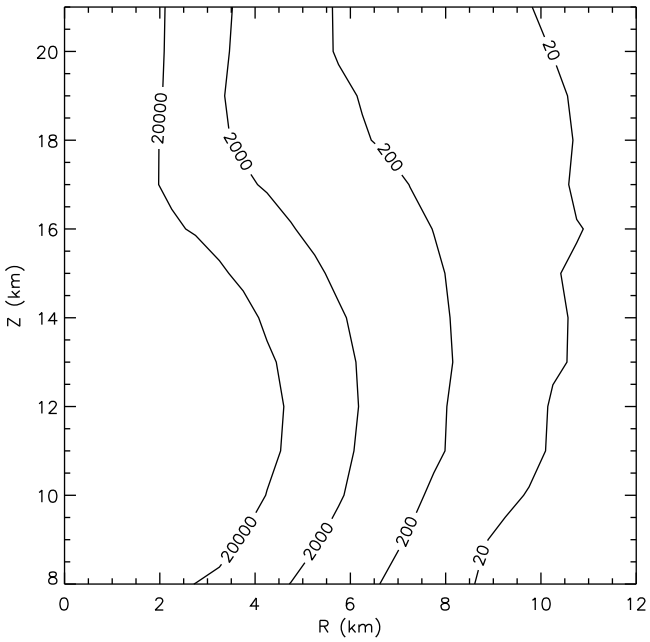


**Figure 8.** Expected total number of counts in ADELE's top and bottom large plastic detectors (>300 keV) in response to a TGF produced at the altitude given on the vertical axis and at a radial distance from the plane given on the horizontal axis, assuming the instrument is between 14.0 and 14.5 km. The TGF is assumed to produce $10^{17}$ photons, an estimate based on observations from space.

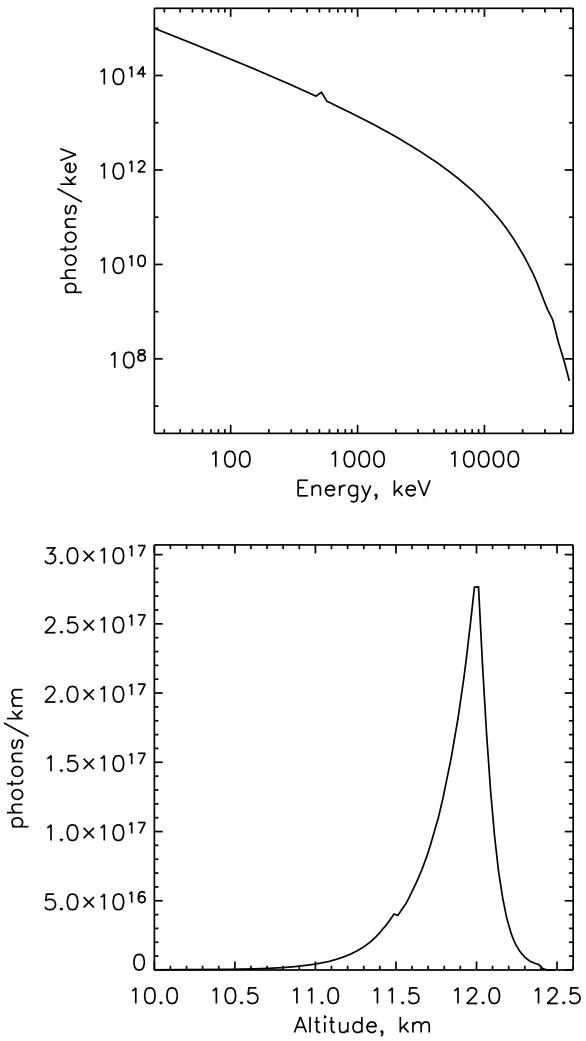


**Figure 9.** Output of the first stage of the TGF simulation (photons produced by the runaway avalanche). (top) Spectral distribution. (bottom) Altitude distribution for the case with the end of the avalanche region fixed at 12 km.

[30] The sequence of Monte Carlo simulation codes used to estimate the number of instrumental counts produced by a TGF (Figure 8) was also used to model the expected top/bottom and (300 keV to 1 MeV)/(>1 MeV) ratios as a function of the production altitude and radial distance of the TGF. Figure 10 shows the simulated top/bottom and spectral ratios expected in ADELE in the GV at 14.1 km altitude as a function of the altitude and distance of the TGF.

[31] Figure 10 (top) shows that the range of possible top/bottom ratios is fairly narrow, making the constraint available from the data not terribly strong; the only parameter space that can be rejected is where the predicted ratio is <0.70, which is where the TGF is directly below the aircraft (within about 1 km radius). It is the highly penetrating nature of the multi-MeV photons that makes it difficult to get extreme top/bottom ratios. A much larger mass of lead shielding between the detectors would make this a more effective diagnostic, but it could still be useful with the instrument as built for a brighter event. With >1000 counts, the difference between a ratio of 0.8 and 1.2, for example, would be clear.

[32] The spectral ratio (300 keV to 1 MeV)/(>1 MeV) in Figure 10 (bottom) is more sensitive. The spectrum is very hard (dominated by the higher-energy band) both above and below the avalanche region, due to the beaming of bremsstrahlung from the electron population upward and the secondary positron population downward. The softest spectra, shown in green, yellow and red, appear directly to the side, at 12–16 km altitude and 1–6 km radial distance. Nearly all this flux has been Compton scattered, often multiple times, lowering its energy into the range of a few hundred keV regardless of the original photon energy. The constraint on this ratio from the data (0.64–2.85 with 95% confidence) rules out a source in this softest region directly to the side of the plane, but no other region is excluded. Furthermore, any significant spreading of the TGF beam, due, e.g., to a diverging electric field, would bring direct

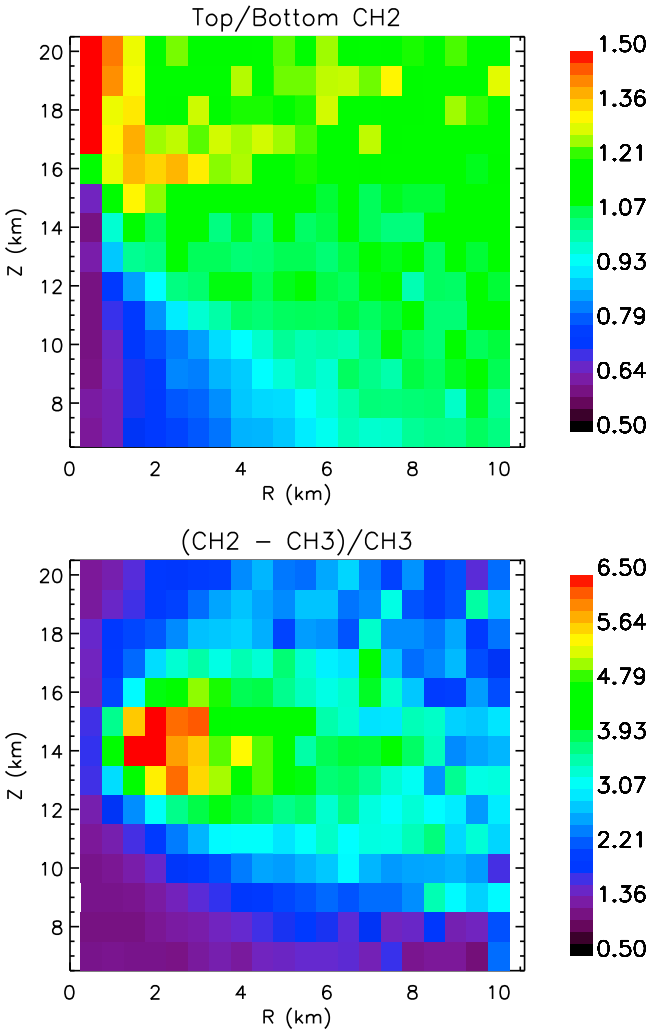


**Figure 10.** Further characteristics of ADELE's response to a TGF as a function of the TGF altitude (vertical axis) and radial distance from the plane (horizontal axis). (top) Ratio of counts >300 keV between the top and bottom detectors. (bottom) Spectral ratio (300 keV to 1 MeV/>1 MeV) using both detectors.

bremsstrahlung photons into this softest region, and probably cause the entire parameter space to become consistent with the range of the spectral ratio from the data.

[33] Since the location of the associated +IC flash gives us a probable location of the TGF, regardless of limits from the gamma ray data alone, it is worth taking a special look at the behavior of Figures 10 (top) and 10 (bottom) at a radial distance of ~10 km. At this distance, both ratios have intermediate values, consistent with the data, for virtually any TGF source altitude. The power of the spectral and directional ratios to determine the TGF source altitude is limited at large distances not just by poor counting statistics but by an intrinsic lack of information in the ratios themselves.

## 4. Summary and Discussion

[34] The first TGF detected from aircraft altitudes was seen on 21 August 2009. Its luminosity, spectral hardness, and upward/downward flux ratio are all consistent with a TGF typical of those seen from space occurring at the center of an active cell ~10 km away. While the gamma ray data alone cannot rule out a much smaller event much closer to the aircraft, a complicated +IC flash produced a series of discharges at the center of this cell that overlapped the time the TGF occurred.

[35] While this detection demonstrates that searching for TGFs near their altitude of origin is feasible, it is clear that more observing time is needed in order to get a significant sample of events. It is also important to fly near storms in the tropics, where the TGF yield observed from space is much higher, to determine whether TGFs are really more frequent in this environment or whether the difference in storm height between midlatitudes and the tropics combined with the atmospheric absorption of gamma rays is the primary driver of the difference between maps of lightning and TGFs observed from space [*Williams et al.*, 2006; *Smith et al.*, 2010; *Splitt et al.*, 2010].

[36] When ADELE or an equally capable instrument eventually detects a TGF from a range of about 5 km or less, the much greater number of photons detected will allow a number of new measurements to be made. This will include the ability to search for fine time structure within the overall TGF pulse and the ability to search, in a single flash, for the high-energy power law spectral component, extending to 100 MeV, reported by *Tavani et al.* [2011] in a spectrum summed over many TGFs seen with AGILE. This spectral component, not yet confirmed by another measurement, is a mystery in terms of the relativistic runaway model, which cannot produce >50 MeV photons without, at the same time, producing orders of magnitude more counts at lower energies than are seen.

[37] **Acknowledgments.** We thank Allen Schanot, the managing scientist of our field campaign from NCAR/EOL; the other NCAR scientists who filled this role earlier or helped us with GV data, Pavel Romashkin, Jorgen Jensen, and Jeff Stith; and the EOL pilots, engineers, and technicians who provided exemplary support. ADELE's construction was funded by NSF major research instrumentation grant ATM-0619941. Our simulation work was supported by NSF grant ATM-0846609. This work includes publicly available data from the KJAX NEXRAD radar of the National Weather Service.

## References

Babich, L. P., E. N. Donskoy, and I. M. Kutsyk (2008), Analysis of atmospheric gamma-ray flashes detected in near space with allowance for the transport of photons in the atmosphere, *J. Exp. Theor. Phys.*, *107*, 49–60.

Briggs, M. S., et al. (2010), First results on terrestrial gamma ray flashes from the Fermi Gamma-ray Burst Monitor, *J. Geophys. Res.*, *115*, A07323, doi:10.1029/2009JA015242.

Carlson, B. E., N. G. Lehtinen, and U. S. Inan (2007), Constraints on terrestrial gamma ray flash production from satellite observation, *Geophys. Res. Lett.*, *34*, L08809, doi:10.1029/2006GL029229.

Cohen, M. B., U. S. Inan, and G. J. Fishman (2006), Terrestrial gamma ray flashes observed aboard the Compton Gamma Ray Observatory/Burst and Transient Source Experiment and ELF/VLF radio atmospherics, *J. Geophys. Res.*, *111*, D24109, doi:10.1029/2005JD006987.

Cohen, M. B., U. S. Inan, R. K. Said, and T. Gjesteland (2010), Geolocation of terrestrial gamma-ray flash source lightning, *Geophys. Res. Lett.*, *37*, L02801, doi:10.1029/2009GL041753.

Connaughton, V., et al. (2010), Associations between Fermi Gamma-ray Burst Monitor terrestrial gamma ray flashes and sferics from the World Wide Lightning Location Network, *J. Geophys. Res.*, *115*, A12307, doi:10.1029/2010JA015681.

Cummer, S. A., Y. Zhai, W. Hu, D. M. Smith, L. I. Lopez, and M. A. Stanley (2005), Measurements and implications of the relationship between lightning and terrestrial gamma ray flashes, *Geophys. Res. Lett.*, *32*, L08811, doi:10.1029/2005GL022778.

Cummer, S. A., G. Lu, M. S. Briggs, V. Connaughton, S. Xiong, G. J. Fishman, and J. R. Dwyer (2011), The lightning-TGF relationship on microsecond timescales, *Geophys. Res. Lett.*, *38*, L14810, doi:10.1029/2011GL048099.

Dwyer, J. R. (2007), Relativistic breakdown in planetary atmospheres, *Phys. Plasmas*, *14*, 042901, doi:10.1063/1.2709652.

Dwyer, J. R., and D. M. Smith (2005), A comparison between Monte Carlo simulations of runaway breakdown and terrestrial gamma-ray flash observations, *Geophys. Res. Lett.*, *32*, L22804, doi:10.1029/2005GL023848.

Eack, K. B., W. H. Beasley, W. D. Rust, T. C. Marshall, and M. Stolzenburg (1996a), Initial results from simultaneous observation of X rays and electric fields in a thunderstorm, *J. Geophys. Res.*, *101*(D23), 29,637–29,640, doi:10.1029/96JD01705.

Eack, K. B., W. H. Beasley, W. D. Rust, T. C. Marshall, and M. Stolzenburg (1996b), X-ray pulses observed above a mesoscale convective system, *Geophys. Res. Lett.*, *23*, 2915–2918, doi:10.1029/96GL02570.

Fishman, G. J., et al. (1994), Discovery of intense gamma-ray flashes of atmospheric origin, *Science*, *264*, 1313–1316.

Grefenstette, B. W., D. M. Smith, J. R. Dwyer, and G. J. Fishman (2007), Time evolution of terrestrial gamma ray flashes, *Geophys. Res. Lett.*, *35*, L06802, doi:10.1029/2007GL032922.

Grefenstette, B. W., D. M. Smith, B. J. Hazelton, and L. I. Lopez (2009), First RHESSI terrestrial gamma ray flash catalog, *J. Geophys. Res.*, *114*, A02314, doi:10.1029/2008JA013721.

Hansen, R. S., N. Østgaard, T. Gjesteland, and J. Stadsnes (2010), Constraints for observing terrestrial gamma-ray flashes by a high-altitude aircraft, *Geophys. Res. Abstr.*, *12*, EGU2010-7882-1.

Hazelton, B. J., B. W. Grefenstette, D. M. Smith, J. R. Dwyer, X.-M. Shao, S. A. Cummer, T. Chronis, E. H. Lay, and R. H. Holzworth (2009), Spectral dependence of terrestrial gamma-ray flashes on source distance, *Geophys. Res. Lett.*, *36*, L01108, doi:10.1029/2008GL035906.

Inan, U. S., S. C. Reising, G. J. Fishman, and J. M. Horack (1996), On the association of terrestrial gamma-ray bursts with lightning and implications for sprites, *Geophys. Res. Lett.*, *23*(9), 1017–1020, doi:10.1029/96GL00746.

Inan, U. S., M. B. Cohen, R. K. Said, D. M. Smith, and L. I. Lopez (2006), Terrestrial gamma ray flashes and lightning discharges, *Geophys. Res. Lett.*, *33*, L18802, doi:10.1029/2006GL027085.

Lu, G., R. J. Blakeslee, J. Li, D. M. Smith, X.-M. Shao, E. W. McCaul, D. E. Buechler, H. J. Christian, J. M. Hall, and S. A. Cummer (2010), Lightning mapping observation of a terrestrial gamma-ray flash, *Geophys. Res. Lett.*, *37*, L11806, doi:10.1029/2010GL043494.

Lu, G., S. A. Cummer, J. Li, F. Han, D. M. Smith, and B. W. Grefenstette (2011), Characteristics of broadband lightning emissions associated with terrestrial gamma ray flashes, *J. Geophys. Res.*, *116*, A03316, doi:10.1029/2010JA016141.

McCarthy, M., and G. K. Parks (1985), Further observations of X-rays inside thunderstorms, *Geophys. Res. Lett.*, *12*, 393–396, doi:10.1029/GL012i006p00393.

Parks, G. K., B. H. Mauk, R. Spiger, and J. Chin (1981), X-ray enhancements detected during thunderstorm and lightning activities, *Geophys. Res. Lett.*, *8*, 1176–1179, doi:10.1029/GL008i011p01176.

Shao, X.-M., T. Hamlin, and D. M. Smith (2010), A closer examination of terrestrial gamma-ray flash-related lightning processes, *J. Geophys. Res.*, *115*, A00E30, doi:10.1029/2009JA014835.

Smith, D. M., L. I. Lopez, R. P. Lin, and C. P. Barrington-Leigh (2005), Terrestrial gamma-ray flashes observed up to 20 MeV, *Science*, *307*, 1085–1088.

Smith, D. M., B. J. Hazelton, B. W. Grefenstette, J. R. Dwyer, R. H. Holzworth, and E. H. Lay (2010), Terrestrial gamma ray flashes correlated to storm phase and tropopause height, *J. Geophys. Res.*, *115*, A00E49, doi:10.1029/2009JA014853.

Smith, D. M., et al. (2011), The rarity of terrestrial gamma-ray flashes, *Geophys. Res. Lett.*, *38*, L08807, doi:10.1029/2011GL046875.

Splitt, M. E., S. M. Lazarus, D. Barnes, J. R. Dwyer, H. K. Rassoul, D. M. Smith, B. Hazelton, and B. Grefenstette (2010), Thunderstorm characteristics associated with RHESSI identified terrestrial gamma ray flashes, *J. Geophys. Res.*, *115*, A00E38, doi:10.1029/2009JA014622.

Stanley, M. A., X.-M. Shao, D. M. Smith, L. I. Lopez, M. B. Pongratz, J. D. Harlin, M. Stock, and A. Regan (2006), A link between terrestrial gamma-ray flashes and intracloud lightning discharges, *Geophys. Res. Lett.*, *33*, L06803, doi:10.1029/2005GL025537.

Tavani, M., et al. (2011), Terrestrial gamma-ray flashes as powerful particle accelerators, *Phys. Rev. Lett.*, *106*, 018501, doi:10.1103/PhysRevLett.106.01851.

Williams, E., et al. (2006), Lightning flashes conducive to the production and escape of gamma radiation to space, *J. Geophys. Res.*, *111*, D16209, doi:10.1029/2005JD006447.

R. J. Blakeslee, NASA Marshall Space Flight Center, 320 Sparkman Dr., Huntsville, AL 35805, USA.

E. Cramer, J. R. Dwyer, H. Rassoul, and M. Schaal, Department of Physics and Space Sciences, Florida Institute of Technology, 150 W. University Blvd., Melbourne, FL 32901, USA.

S. A. Cummer and G. Lu, Electrical and Computer Engineering Department, Duke University, PO Box 90291, Durham, NC 27708, USA.

B. W. Grefenstette, Space Radiation Laboratory, California Institute of Technology, Pasadena, CA 91125, USA.

T. Hamlin, C. Ho, and X.-M. Shao, Los Alamos National Laboratory, ISR-2, MS D436, Los Alamos, NM 87545, USA.

B. J. Hazelton, Department of Physics, University of Washington, Box 351560, Seattle, WA 98195, USA.

S. Heckman, AWS Convergence Technologies, Inc., 12410 Milestone Center Dr., Germantown, MD 20876, USA.

N. A. Kelley, G. F. M. Martinez-McKinney, D. M. Smith, and Z. Y. Zhang, Santa Cruz Institute for Particle Physics, Physics Department, University of California, 1156 High St., Santa Cruz, CA 95064, USA. (dsmith@scipp.ucsc.edu)

S. M. Lazarus and M. E. Splitt, Department of Marine and Environmental Systems, Florida Institute of Technology, 150 W. University Blvd., Melbourne, FL 32901, USA.

A. W. Lowell, Space Sciences Laboratory, University of California, 7 Gauss Way, Berkeley, CA 94720, USA.

Z. H. Saleh, Department of Medical Physics, Memorial Sloan-Kettering Cancer Center, 1275 York Ave., New York, NY 10065, USA.

W. Ulrich, National Weather Service WFO Key West, 1315 White St., Key West, FL 33040, USA.